CAMBRIDGE
UNIVERSITY PRESS

Standard Paper

Chromosomal genome sequence assembly and mating-type (*MAT*) locus characterization of the leprose asexual lichenized fungus *Lepraria neglecta* (Nyl.) Erichsen

Bubba Pfeffer[1], Chandler Lymbery[1], Brendan Booth[1] and Jessica L. Allen[1] (ID)

[1]Department of Biology, Eastern Washington University, Cheney, WA, USA

Abstract

Complete chromosomal-level assemblies of fungal genomes are rare. The intimate ecological symbioses and complex reproduction strategies utilized by fungi make highly contiguous, gapless genome assemblies particularly difficult. Here, we use long-read sequencing on the Oxford Nanopore Technology MinION platform to sequence and assemble the genome of *Lepraria neglecta* (*Ascomycota*, *Lecanorales*). In addition to eight contigs ascribable to chromosomes, six of which are assembled telomere-to-telomere, we discovered the presence of a complete *MAT* locus with two conserved *MAT1-2* genes and a putative *MAT1-1* pseudogene. The full genome assembly of a widespread, common species presents an opportunity for new insights into lichen reproduction while the presence of the mating-type locus in the genome of an asexual lichen raises fundamental questions about reproductive biology in fungi generally.

Key words: asexual reproduction, chromosome assembly, chromosome counts, fungal mating systems

(Accepted 3 November 2022)

Introduction

Complete fungal genomes, those assembled to gapless full chromosomes, are uncommon. This level of completion is mostly restricted to well-studied, model species, such as *Aspergillus oryzae* (Ahlb.) Cohn, *Fusarium* spp. and *Penicillium chrysogenum* Thom (Machida *et al.* 2005; Specht *et al.* 2014; King *et al.* 2015, 2018), although there are an increasing number of non-model fungi with telomere-to-telomere assemblies available (Chung *et al.* 2021; Crestana *et al.* 2021; Gan *et al.* 2021). The scarcity of full chromosome assemblies of fungal genomes partially stems from the difficulty in obtaining pure samples. Many fungi are unculturable (Muggia *et al.* 2017; Tedersoo *et al.* 2018). Furthermore, they are typically involved in complex, intimate symbioses (Smith & Read 2008; Stajich *et al.* 2009) and can be inseparable from their symbionts. Because fungi are often embedded in diverse microbial communities, whole-genome shotgun sequencing of environmental samples yields rich and complex metagenomes that can be challenging to analyze (Grube *et al.* 2013; Keepers *et al.* 2019; Tzovaras *et al.* 2020). Despite these challenges, a number of nearly complete lichen genomes have been published (Table 1). In the immediate future, highly complete genomes are poised to become the norm as widespread adoption of long-read sequencing methods expands our data generation capacity (McKenzie *et al.* 2020; Tedersoo *et al.* 2021).

Fungi, especially in the phylum *Ascomycota*, demonstrate some of the most diverse strategies for reproduction of all eukaryotes that span the full spectrum of recombination from obligate outcrossing to clonality (Tripp 2016; Kendrick 2017). Heterothallism involves the fusion of genetically distinct individuals expressing different mating types (Billiard *et al.* 2012). Heterothallism is exceedingly common among lichen-forming fungi and is most likely the ancestral state for *Lecanoromycetes* (Pizarro *et al.* 2019). Homothallism represents a diverse and varied set of strategies utilized by fungi to allow for self-fertility (Wilson *et al.* 2015b). Fungi exhibiting primary homothallism are capable of expressing both *MAT1-1* and *MAT1-2* idiomorphs in a single genome. Pseudohomothallic fungi produce dikaryotic spores which contain two nuclei, each expressing a complementary *MAT* idiomorph. Other homothallic fungi are capable of hermaphroditic mating-type switching, so that individuals can swap which *MAT* idiomorph is expressed in their genome. Unisexuality represents a unique, perhaps separate kind of homothallism, identified in only four fungal species to date (Wilson *et al.* 2021). The unisexual fungus *Cryptococcus neoformans* (San Felice) Vuill., for instance, is capable of sexual meiosis by whole-genome endoreplication or by cellular and nuclear fusion of two individuals of the same *MAT* identity (Wilson *et al.* 2021). These examples of homothallism all involve sexual meiosis of identical clones and the potential to recombine with oneself and every other individual of the same species (Billiard *et al.* 2012). Strictly asexual organisms reproduce exclusively through clonal spores or vegetative tissue adapted to facilitate fragmentation and dispersal. Throughout domain *Eukarya*, asexual reproduction is frequently observed in conjunction with facultative

CrossMark

Table 1. Assembly metrics for several highly-complete lichenized fungal genomes, including the *Lepraria neglecta* genome presented here (in bold). Metrics were calculated with Quast v. 5.0.2 (Mikheenko *et al.* 2018) and BUSCO v. 5 (Manni *et al.* 2021). BUSCO scores show the number of genes and the percentage in parentheses. GC content represents the percentage of nucleotides that are guanines and cytosines in the total sequence assembly. N50 is a measure of contiguity; it is the length of the shortest contig in the group of the longest contigs which together represent 50% of the assembly. L50 is the smallest number of contigs that includes 50% of the total sequence assembly length.

Species	Total length (Mb)	Scaffold/contig no.	N50 (Mb)	L50	GC Content	BUSCO complete single	BUSCO complete duplicate	BUSCO incomplete	BUSCO missing	Reference
Bacidia gigantensis	33.1	0 / 24	18.1	8	44.67%	1186 (92.7%)	1 (0.5%)	35 (2.6%)	35 (4.6%)	Allen *et al.* (2021)
Cladonia grayi	34.6	414 / 538	0.24	43	44.44%	1647 (96.6%)	8 (0.5%)	11 (0.6%)	48 (2.8%)	Armaleo *et al.* (2019)
C. macilenta	37.1	240 / 1125	1.47	11	44.68%	1653 (96.9%)	12 (0.7%)	6 (0.4%)	47 (2.7%)	Park *et al.* (2013a)
C. straminea	36.7	30 / 623	1.59	10	44.91%	1650 (96.7%)	8 (0.5%)	9 (0.5%)	47 (2.8%)	Park *et al.* (2014a)
Evernia prunastri	40.3	277 / 567	0.26	51	48.97%	1649 (97.2%)	16 (0.9%)	8 (0.5%)	39 (2.3%)	Meiser *et al.* (2017)
Gyalolechia flavorubescens	34.5	36 / 142	1.69	9	41.89%	1658 (97.2%)	5 (0.3%)	9 (0.5%)	39 (2.3%)	Park *et al.* (2013b)
Lepraria neglecta	**42.1**	**0 / 11**	**5.20**	**4**	**47.38%**	**1652 (96.85%)**	**12 (0.7%)**	**6 (0.4%)**	**36 (2.1%)**	**Reported here**
Letharia columbiana	52.3	0 / 161	0.67	23	39.58%	1637 (92.3%)	62 (3.6%)	10 (0.6%)	59 (3.5%)	McKenzie *et al.* (2020)
L. lupina	49.2	0 / 31	2.10	10	38.73%	1649 (96.0%)	12 (0.7%)	6 (0.4%)	51 (2.9%)	McKenzie *et al.* (2020)
Pseudevernia furfuracea	37.8	46 / 142	1.18	10	47.86%	1648 (96.2%)	7 (0.4%)	6 (0.4%)	52 (3.0%)	Meiser *et al.* (2017)
Ramalina intermedia	26.2	196 / 207	0.27	31	51.89%	1635 (95.9%)	6 (0.4%)	12 (0.7%)	59 (3.4%)	Wang *et al.* (2018)
Umbilicaria muehlenbergii	34.8	7 / 278	7.01	2	47.12%	1643 (95.5%)	13 (0.8%)	29 (1.7%)	34 (2.0%)	Park *et al.* (2014b)

sexual outcrossing (Honnay & Bossuyt 2005). Many species of fungi are called 'imperfect' because they have never been observed exhibiting a sexual stage, and as such might be examples of strictly exclusive asexuals (Gräser *et al.* 1999; Persinoti *et al.* 2018). Furthermore, it is important to recognize that the reproductive categories listed here are artificial creations, constructs of scientific theory. Fungal reproduction exists along poorly understood spectra, and species are not restricted to one category. For example, the polymorphic fungus *Candida albicans* (C.P. Robin) Berkhout is capable of heterothallic and unisexual reproduction, as well as parasexual reproduction, a process of ploidy reduction via concerted chromosome loss rather than meiosis (Bennett & Johnson 2003; Thomson *et al.* 2019; Wilson *et al.* 2021).

Lepraria s. lat. is a chemically and morphologically diverse genus of *c.* 60 species of leprose lichens (Lendemer 2013; Lendemer & Hodkinson 2013). *Lepraria* species have never been observed with sexual reproductive structures (Lendemer 2013), and *Lepraria* is thus assumed to be exclusively clonal. Clonal reproduction is assumedly accomplished through the leprose growth form, which consists entirely of ecorticate granules that function simultaneously as the lichen thallus and as dispersal propagules (Brodo 2001). *Lepraria* makes effective use of the vegetative mode of reproduction, vertically transmitting the entire holobiome between indiscreet generations. Interestingly, phylogenetic studies of *Lepraria* based on typical species-level molecular markers result in phylogenies with short branch lengths and poor support for species that are clearly morphologically, chemically and geographically distinct (Lendemer & Hodkinson 2013), suggesting evolutionary processes in this genus do not mirror those observed in other lineages of lichenized fungi. While leprose thalli have arisen in other lineages of lichenized fungi, including genera such as *Chrysothrix*, *Lecanora* and *Herpothallon*, no other lineages exhibit the same degree of strictly asexual diversification as *Lepraria* (Lendemer 2013). Therefore, *Lepraria* is an ideal genus for investigating reproductive strategies and their evolutionary outcomes.

In the present study, long-read sequence data were used from the Oxford Nanopore MinION platform to sequence the genome of *Lepraria neglecta* (Nyl.) Erichsen, a widespread species with a nearly global distribution. It is distinguished within the genus by its unparalleled chemical variation (i.e. there are at least seven distinct chemotypes with overlapping ranges; Lendemer 2013). The nuclear and mitochondrial genomes of *L. neglecta*, and the organellar genomes of the photobiont, were assembled from the complex metagenomic data that resulted from a whole thallus extract. A detailed investigation of the genome assembly was conducted to locate telomeres and the mating-type locus, and to infer the number of chromosomes.

Materials and Methods

Sample collection, DNA extraction and sequencing

Lepraria neglecta was collected 330 m south-east of the Cheney Wastewater Treatment Plant and 600 m north-east of the Columbia Plateau Trailhead (47.4823°N, 117.5555°W). All tissue was taken from a single thallus occupying a rock outcrop and the thallus was removed from the substratum with a sterile butter knife. Collectors wore nitrile gloves during the collection process and samples were placed in new paper bags to avoid contamination. Samples were taken back to the laboratory and placed in a −20 °C freezer. The thallus was removed from the freezer 24

h later, cleaned of debris, and divided into 16 1.5 ml tubes. The sample voucher specimen was deposited in the Eastern Washington University herbarium (EWU; *Allen* 5258). Thin-layer chromatography was conducted using a small subset of the sample following standard methods (Culberson & Kristinsson 1970). Metabolites were extracted with acetone and transferred to an aluminum-backed silica plate with 250 nm fluorescent markers (Merck KGaA, Darmstadt, Germany). The plate was run in solvent C (200 toluene: 30 glacial acetic acid), and fluorescence of metabolites under short- and long-wave ultraviolet light was recorded. The plate was then treated with water and the presence of hydrophobic spots was marked as the plate dried. Once the plate was dry, it was treated with 10% sulphuric acid and heated on a pancake griddle at 200° F (*c.* 93 °C) for 15 min before final interpretation.

The Qiagen DNEasy PlantPro Kit was used for DNA extraction following the manufacturer's protocol with one adjustment: tissue disruption using a Mini-BeadBeater Mill 36270-02 was completed before the addition of any solutions (Qiagen, Hombrechtikon, Switzerland). Extractions were eluted in 50 μl of the elution buffer, all 16 extractions were pooled, and total DNA was quantified using a Qubit with ssDNA Assay Kit (Invitrogen, Waltham, MA, USA). A size selection step using MagBind Total Pure NGS (Omega Bio-tek, Inc., Norcross, GA, USA) was then completed with a 0.4:1 bead solution to extract ratio, a series of 70% ethanol washes were carried out, and the sample was eluted in 55 μl of nuclease-free water (McKenzie *et al.* 2020). Library preparation was completed using the Ligation Sequencing Kit LKS-109 according to the manufacturer's protocol and samples were run on the MinION platform using R.9.4.1 flow cells for 52 h (Oxford Nanopore Technologies, Oxford, UK). Basecalling was conducted using Guppy v. 5.0.7 with the SUP model (Oxford Nanopore Technologies, Oxford, UK).

Genome assembly and filtering

Reads were assembled using Flye v. 2.9 with the '--nano-hq' mode, read error set to 0.02 and maximum overhang set to 250 (Kolmogorov *et al.* 2019). The resulting assembly was polished with medaka v. 1.2 after mapping all reads back to assembled contigs using minimap2 v. 2.17 (Li 2018; https://github.com/nano-poretech/medaka). Linear contigs with > 60× coverage ascribable to *Ascomycota* using the metagenomic binning methods in McKenzie *et al.* (2020) were retained for downstream analyses as the nuclear genome of *Lepraria neglecta*. Circular contigs ascribable to *Ascomycota* were retained as potential mitochondrial genomes and circular contigs ascribable to *Chlorophyta* were retained as potential photobiont organellar genomes. Quast v. 5.0.2 and BUSCO v. 5 were used to calculate final assembly metrics for *L. neglecta* and a suite of other lichen species for comparison (Mikheenko *et al.* 2018; Manni *et al.* 2021; Table 1). Reads were also assembled with Flye v. 2.9 with the '--meta' mode to recover the photobiont mitochondrial genome (Kolmogorov *et al.* 2019). High-coverage circular contigs were searched against the NCBI nucleotide database using BLASTN to recover the contigs ascribable to the *Trebouxiophyceae*. Organellar genomes were annotated with GeSeq on the CHLOROBOX platform hosted by the Max Planck Institute of Molecular Plant Physiology (Supplementary Material Fig. S1, available online; Tillich *et al.* 2017).

Nuclear genome contigs were annotated with funannotate v. 1.8.7 (https://github.com/nextgenusfs/funannotate). All default

ab-initio and evidence-based predictors were used and protein evidence was derived from the following Joint Genome Institute databases: *Cladonia grayi* Cgr/DA2myc/ss v2.0, *Lobaria pulmonaria* Scotland reference genome v1.0, *Usnea florida* ATCC18376 v1.0, *Xanthoria parietina* 46-1-SA22 v1.1, and complete MAT loci from *Letharia vulpina* (GenBank: MK521632.1) and *Letharia columbiana* (GenBank: MK521629.1). BUSCO searches were conducted with *Aspergillus fumigatus* Fresen. as the seed species. Biosynthetic gene clusters were annotated with antiSMASH v. 6.0 (Blin *et al.* 2021).

Telomeres were identified using a custom set of scripts (Supplementary Material File S1, available online). Reads were searched for telomeric repeats (TTAGGG in most fungi) using the Noise Cancelling Repeat Finder (Harris *et al.* 2019). Reads with ≥ 60 bp stretches with ≥ 95% identity to the repeated telomeric repeat motif within 40 bp of the beginning or end of the read (to allow for adapter sequence) were annotated as telomeric. Reads with telomeric sequences were then mapped to the assembly graph using GraphAligner with the following parameters: ard-cigar --seeds-mxm-length 30 --seeds-mem-count 10000 --bandwidth 15 --multimap-score-fraction 0.999 --precise-clipping 0.85 --min-alignment-score 5000 --clip-ambiguous-ends 100 --overlap-incompatible-cutoff 0.15 --max-trace-count 5 (Rautiainen & Marschall 2020). The assembly graph was then examined along with the results of GraphAligner to determine which graph edges were fully connected to each other with telomeric reads, and these results were used to create a visual representation of the results in Inkscape v. 1.2.1 (Fig. 1; https://inkscape.org/). The assembly graph and results of GraphAligner are available in text form in Supplementary Material File S2 (available online). Contigs with telomeric reads mapping to both ends are considered telomere-to-telomere assembled chromosomes. As a point of comparison, this same workflow was used to map telomeric reads in *Bacidia gigantensis* Lendemer *et al.* (Allen *et al.* 2021).

To confirm that this sample is *Lepraria neglecta* and determine which individuals with available sequences are most closely related to our sample, we built a single-gene phylogeny using the nuclear internal transcribed spacer (ITS). The ITS sequence of this sample was recovered from the genome assembly using a BLASTN search with a *L. neglecta* isolate (GenBank #KC209167.1, *Lendemer* 16108 (NY), alectorialic acid chemotype) ITS sequence as the query (Altschul *et al.* 1990). The recovered ITS sequence from the genome presented here was then queried against the entire NCBI nucleotide database using BLASTN; 453 ITS sequences were recovered as the closest hits and downloaded. These sequences were then aligned with MUSCLE v. 5 and the resulting alignment was visualized and cleaned using Jalview v. 2.11.2.0 (Clamp *et al.* 2004; Edgar 2021). Sequences that did not align, which were substantially shorter than the majority of sequences in the dataset, or that appeared to be potential misidentifications were removed. Remaining sequences were then realigned using MUSCLE v. 5. That alignment was then used as the input for IQ-TREE v. 2.0.3 to conduct maximum likelihood phylogenetic inference with 1000 bootstrap replicates, implementing the ModelFinder Plus option (Nguyen *et al.* 2015; Kalyaanamoorthy *et al.* 2017). We identified clades for *Lepraria atlantica* Orange, *L. granulata* Slav.-Bay., *L. humida* Slav.-Bay., *L. neglecta* and *L. straminea* Vain., using *L. elobata* Tønsberg as the outgroup. All other sequences were removed from the dataset and the remaining 82 sequences were realigned in MUSCLE v. 5; a second phylogeny was built using these sequences and the settings in IQ-TREE v. 2.0.3 as described

above. The phylogeny was visualized in FigTree v. 1.4.4 and the final phylogeny figure was edited in Adobe Illustrator.

Annotating the mating-type locus

To search for *MAT* genes in the *Lepraria neglecta* genome, we used BLASTP to search the annotations with previously published *MAT* locus genes as queries. The final set of amino acid sequence annotations from funannotate were used to create a blast database (Altschul *et al.* 1990). The complete mating-type loci from *Letharia vulpina* strain U042 (GenBank Accession MK521632.1), which includes *APN2, MAT1-1-7, MAT1-1-1*, an open reading frame, and *SLA2* genes, and *Letharia columbiana* strain U080 (GenBank Accession MK521629.1), which includes

APN2, MAT1-2-1, MAT1-2-14, an open reading frame and *SLA2* genes, were then used as queries in BLASTP searches against the database of all annotations from *L. neglecta* (Ament-Velásquez *et al.* 2021). The complete nucleotide sequence of the *L. neglecta* genome was converted to a blast database and TBLASTN was used to search the genome along with the same set of *Letharia* queries as above. The resulting *L. neglecta* annotations and DNA sequences that were best matches to the *Letharia* mating-type genes were then used to conduct a reciprocal blast search against the entire NCBI nucleotide database to confirm that there were no other, more similar sequences. The relative location of all recovered annotation and sequence matches were visually examined using IGV (Thorvaldsdóttir *et al.* 2013).
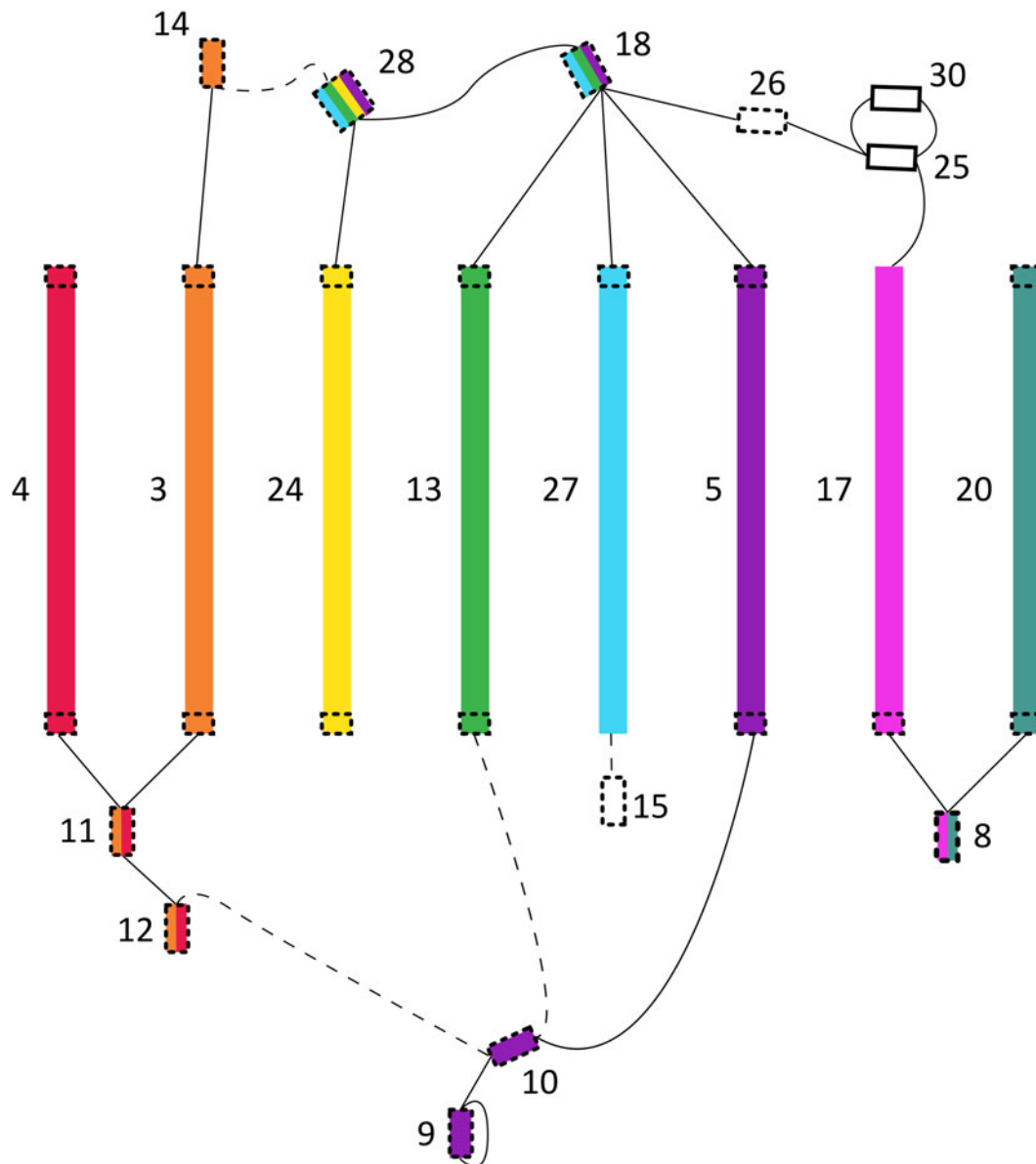

Fig. 1. Representation of the assembly graph for the *Lepraria neglecta* nuclear genome assembly showing the eight large contigs ascribable to full chromosomes, each of which is assigned a unique colour/shade. Each rectangle represents a graph edge and the numbers next to the rectangles correspond to the graph edge number. Locations where telomeric reads are mapped are indicated by boxes with dashed edges. Solid lines connecting rectangles represent paths that are confirmed based on telomeric read mapping. Two rectangles connected by a solid line indicates that telomeric reads are mapped to the ends of the rectangles on either side of the line. Dashed lines indicate paths that were not supported by telomeric reads spanning both edges. In colour online.

Table 2. Summary of contigs ascribable to chromosomes, assembled for *Lepraria neglecta*. All contigs were assembled with Flye v. 2.9 (Kolmogorov *et al.* 2019) with the '--nano-hq' mode except the *Asterochloris* mitochondrial genome, for which the '--meta' mode was used. Coverage values were recorded from the assembly statistics.

Contig no.	Chromosome name	Length (bp)	Coverage (x)	Structure	Identity	Telomeric reads on left end	Telomeric reads on right end	Short, contains telomeric reads
17	I	6292759	99	linear	nuclear	No	Yes	N/A
5	II	5984617	100	linear	nuclear	Yes	Yes	N/A
4	III	5326241	100	linear	nuclear	Yes	Yes	N/A
20	IV	5200541	100	linear	nuclear	Yes	Yes	N/A
3	V	4931745	100	linear	nuclear	Yes	Yes	N/A
24	VI	4758479	99	linear	nuclear	Yes	Yes	N/A
13	VII	4732969	102	linear	nuclear	Yes	Yes	N/A
27	VIII	4487613	99	linear	nuclear	No	Yes	N/A
15	N/A	172877	87	linear	nuclear	N/A	N/A	Yes
26	N/A	101587	88	linear	nuclear	N/A	N/A	Yes
12	N/A	26033	62	linear	nuclear	N/A	N/A	Yes
N/A	N/A	209554	57	circular	*Asterochloris* chloroplast	N/A	N/A	N/A
N/A	N/A	83500	20	circular	*Asterochloris* mitochondrial	N/A	N/A	N/A
N/A	N/A	52980	24	circular	*Cladonia* mitochondrial	N/A	N/A	N/A
N/A	N/A	38898	913	circular	*L. neglecta* mitochondrial	N/A	N/A	N/A

Results

Eight contigs ascribable to chromosomes were assembled for *L. neglecta* (Fig. 1, Table 2). Six of the contigs were assembled telomere-to-telomere. Two contigs did not assemble through telomeres on one end but are adjacent to graph edges with telomeric sequences in the assembly graph. The assembly graph for contig 27 shows a potential connection with contig 15, which does contain telomeric sequences, though no telomeric reads connecting the two contigs were recovered. The assembly at the left end of contig 17 was not resolvable through subtelomeric repeats. Three additional small contigs were assembled, two of which were comprised of telomeric and subtelomeric repeats that were not able to be assembled with confidence at the ends of large contigs (contigs 26 and 15; see edges 26 and 15 in Fig. 1), and one which was a small, lower coverage repetitive element that clearly represents an assembly artifact (contig 12). The assembly size of the mycobionts fell within the previously documented size range of lichenized fungi (41.7 Mb, 100× coverage; Table 1). The assembly was highly contiguous (*L. neglecta* N50 = 5.202 Mbp, L50 = 4) and highly complete (97.5% of BUSCO genes were recovered). N50 refers to the length of the shortest contig in the group of the longest contigs which together represent 50% of the assembled genome. L50 is the smallest number of contigs that includes 50% of the total sequence assembly length. A total of 14 734 genes were predicted for *L. neglecta* with funannotate v. 1.8.7 (Table 3). The whole mitochondrial genome was recovered from the mycobiont (Supplementary Material Fig. S1, available online: 38 898 bp, 913× coverage). In addition, a low

Table 3. Annotation results of predicted gene categories for *Lepraria neglecta* from funannotate v. 1.8.7 (https://github.com/nextgenusfs/funannotate) and antiSMASH v. 6.0 (Blin *et al.* 2021). A total of 14 734 genes were predicted. Gene categories include transfer RNAs (tRNA), Carbohydrate-Active Enzymes (CAZymes), biosynthetic gene clusters (antiSMASH clusters), biosynthetic enzymes (antiSMASH biosynthetic enzymes) and secondary metabolite gene families (smCOGs).

Category	Count
Total gene models	14 734
tRNA	43
CAZymes	237
antiSMASH clusters	48
antiSMASH biosynthetic enzymes	118
antiSMASH smCOGs	146

coverage assembly of a mitochondrion that most closely matches *Cladonia* in a homology search was also recovered (52 980 bp, 24× coverage, closest match *Cladonia stipitata* GenBank Accession AVT43930). The chloroplast genome from the photobiont, which most closely matches *Asterochloris* sp. Armaleo s. n. sequence ID: JN573844.1 (Thüs *et al.* 2011), was also assembled and annotated (209 823 bp, 57× coverage), as was the photobiont mitochondrial genome (83 500 bp, 20× coverage). Telomeric read mapping of the *Bacidia gigantensis* genome resulted in 10 contigs with telomeric reads mapped to both ends, 13 contigs with telomeric reads mapped to one end, and the one

Fig. 2. A diagram representing the relative location and direction of genes in the *MAT* locus of *Lepraria neglecta*. * and dashed line indicate a pseudogene. The *MAT1-2-x* and *MAT1-1-x* were recovered through BLAST searches against *Letharia* spp. *MAT1-2-14* and *MAT1-1-1* genes, respectively (Table 4). The final numeral is assigned to *x* because of uncertainty with respect to a more specific identity. In colour online.

Table 4. Summary of the BLAST search for *MAT1* genes, including information on the query and subject sequences, and metrics from each BLAST result. Query genes include one long open reading frame (LORF).

Query gene	Query protein ID	Query species	Subject sequence type	Annotation result	% identity	e-value
*APN*2	QEL51145.1	*Letharia vulpina*	Genome-wide annotated amino acids	OEA41_005823	73%	0
*APN*2	QEL51131.1	*Letharia columbiana*	Genome-wide annotated amino acids	OEA41_005823	74%	0
LORF	QEL51146.1	*Letharia vulpina*	Genome-wide annotated amino acids	no hits found	no matches	no matches
LORF	QEL51132.1	*Letharia columbiana*	Genome-wide annotated amino acids	no hits found	no matches	no matches
MAT1-2-1	QEL51133.1	*Letharia columbiana*	Genome-wide annotated amino acids	OEA41_005822	44%	2.00E-104
MAT1-2-14	QEL51134.1	*Letharia columbiana*	Genome-wide annotated amino acids	OEA41_005821	51%	4.00E-41
MAT1-1-1	QEL51148.1	*Letharia vulpina*	Genome-wide annotated amino acids	no hits found	no matches	no matches
MAT1-1-1	QEL51148.1	*Letharia vulpina*	*MAT* locus nucleotides	NA	53%	5.00E-17
MAT1-1-7	QEL51147.1	*Letharia vulpina*	Genome-wide annotated amino acids	no hits found	no matches	no matches
MAT1-1-7	QEL51147.1	*Letharia vulpina*	*MAT* locus nucleotides	no hits found	no matches	no matches
SLA2	QEL51149.1	*Letharia vulpina*	Genome-wide annotated amino acids	OEA41_005820	91%	0
SLA2	QEL51135.1	*Letharia columbiana*	Genome-wide annotated amino acids	OEA41_005820	91%	0

scaffold with no telomeric reads mapping (Supplementary Material File S2, available online).

Taxonomic placement of the *Lepraria neglecta* specimen was confirmed with a maximum likelihood phylogeny of the ITS sequences of closely related *Lepraria* species (Supplementary Material Fig. S2, available online). Interestingly, the present individual demonstrated 100% ITS sequence identity with a member of the stictic acid chemotype collected from Yosemite National Park, California (GenBank #|KC209133, *Lendemer* 19632 (NY)). The sample sequenced here was determined by TLC to be the roccelic acid chemotype.

A mating-type locus was identified in the *Lepraria neglecta* genome, characterized by peripheral *APN2* and *SLA2* genes, oriented inwards (Fig. 2, Table 4). Complete genes were found for *MAT1-2-1* and *MAT1-2-14* (44% sequence identity, 1179 bp and 51% sequence identity, 630 bp, respectively, to GenBank Accession MK521629.1). A tblastn search of the *Letharia vulpina* *MAT1-1-1* amino acid sequence (GenBank Accession MK521632.1) against the nucleotide sequence of the mating-type region in *Lepraria neglecta* resulted in a match of 472 bp with 53% sequence identity and e-value of 5e-17. The translation of this nucleotide sequence to amino acids revealed multiple internal stop codons. Based on the low similarity and the truncation of the *Lepraria neglecta* sequence, we opted to refer to this as a putative *MAT1-1-x* pseudogene since we cannot confidently assign it to a subtype of *MAT1-1* genes. No significant blast hits were recovered for the *Letharia vulpina* long open reading frames (LORF) or for *MAT 1-1-7*. Reciprocal blastp searches of the entire NCBI nucleotide database resulted in these same genes being recovered as the best matches. Sequence synteny and orientation

of the *MAT* locus was consistent with other species of *Ascomycota* (Pizarro *et al.* 2019; Ament-Velásquez *et al.* 2021).

Discussion

The *Lepraria neglecta* genome assembly presented here, being complete and contiguous telomere-to-telomere for nearly every chromosome, represents a major advancement in resources for the study of fungi. Our results suggest that the *L. neglecta* genome is organized into eight chromosomes, and we successfully mapped telomere sequences to both ends of six of the eight chromosomes and to one end of two of the eight (Fig. 1). One of the contigs for which telomeres were not mappable to one end was the longest contig of the assembly (6 292 759 bp) and the assembly is not fully resolved through the subtelomeric repeats on one end of the contig into the telomere region. The other contig lacking a telomere on one end was also large (4 487 623 bp) and adjacent to a telomeric graph edge, though no reads spanned from the telomere into the contig. Thus, we are confident that this is a near-full chromosome contig that will be resolvable through both telomeres with the acquisition of additional data. By comparison, this same telomere analysis of the Allen *et al.* (2021) *Bacidia gigantensus* genome assembly recovered 10 contigs that included telomeres on both ends, 13 that included telomeres on one end and one scaffold that included no telomeres (see assembly graph and mapped telomeric reads in Supplementary Material File S2, available online). An assembly of the *Umbilicaria pustulata* (L.) Hoffm. genome from long-read data recovered 7 scaffolds, which may represent chromosomes once telomere mapping is conducted (Tzovaras *et al.* 2020). Our chromosome

Table 5. Summary of chromosome counts from diverse fungal taxa. The number of chromosomes represents the total range of numbers reported from all species studied in each order (see also Supplementary Material File S2, available online).

Phylum	Order	No. of chromosomes	Reference
Ascomycota	*Acarosporales*	3	Altman & Dittmer ([1972](#))
	Caliciales	4	Altman & Dittmer ([1972](#))
	Capnodiales	5	Wang *et al.* ([2020](#))
	Diaporthales	4	Tischler ([1922](#))
	Dothideales	21	Goodwin *et al.* ([2011](#))
	Eurotiales	4–8	Altman & Dittmer ([1972](#)); Machida *et al.* ([2005](#)); Specht *et al.* ([2014](#))
	Geoglossales	8	Tischler ([1922](#))
	Glomerellales	7	Altman & Dittmer ([1972](#))
	Hypocreales	4–7	Altman & Dittmer ([1972](#)); King *et al.* ([2015](#), [2018](#)); Kramer & Nodwell ([2017](#)); Olarte *et al.* ([2019](#))
	Hysteriales	4	Altman & Dittmer ([1972](#))
	Laboulbeniales	4	Tischler ([1922](#))
	Lecanorales	3–6	Altman & Dittmer ([1972](#))
	Microascales	4	Altman & Dittmer ([1972](#))
	Onygenales	4–16	Altman & Dittmer ([1972](#))
	Pertusariales	5–7	Altman & Dittmer ([1972](#))
	Pezizales	4–18	Tischler ([1922](#)); Altman & Dittmer ([1972](#))
	Pleosporales	4	Tischler ([1922](#))
	Rhytismatales	5	Altman & Dittmer ([1972](#))
	Sordariales	7	Altman & Dittmer ([1972](#))
	Verrucariales	4–8	Tischler ([1922](#)); Altman & Dittmer ([1972](#)); Patwardhan & Badhe ([1978](#))
	Xylariales	4–7	Altman & Dittmer ([1972](#))
Basidiomycota	*Acarosporales*	3	Altman & Dittmer ([1972](#))
	Agaricales	3–16	Stajich *et al.* ([2009](#))
	Auriculariales	8	Altman & Dittmer ([1972](#))
	Cantharellales	6	Altman & Dittmer ([1972](#))
	Microbotryales	10–12	Altman & Dittmer ([1972](#))
	Pucciniales	3–8	Altman & Dittmer ([1972](#))
	Russulales	7	Altman & Dittmer ([1972](#))
	Tremellales	14–16	Altman & Dittmer ([1972](#)); D'Souza *et al.* ([2011](#)); Janbon *et al.* ([2014](#))
Blastocladiomycota	*Blastocladiales*	14–28	Altman & Dittmer ([1972](#))

count falls well within the range of previously published literature reporting 2–21 chromosomes in diverse species of fungi ([Table 5](#); Supplementary Material File S2). Flow cytometry is the preferred method for measuring genome size and chromosome number due to its accuracy and precision (D'hondt *et al.* 2011; Talhinhas *et al.* 2017), but it is not always feasible to implement (Poma *et al.* 1998). Short-read genome assemblies are inaccurate and imprecise for measuring genome size and inferring chromosome numbers in comparison to flow cytometry (Kooij & Pellicer 2020). In contrast, highly complete genome assemblies from long-read sequencing data are one approach to more accurately infer chromosome numbers without flow cytometry. The success of using genome assemblies to infer chromosome numbers may be inconsistent since chromosome numbers among cells in the same fungus can vary, as shown in an early account of meiosis in *Neottiella rutilans* (Fr.) Dennis (Rossen & Westergaard 1966). However, given a sample with homogenous chromosome counts, long-read data has proved useful for telomere-to-telomere assemblies.

Mating-type locus

The conservation of a complete mating-type locus, including multiple *MAT1-2* genes in a lichenized fungal lineage that has never been observed to produce sexual reproductive structures, raises questions about reproduction in putatively asexual lichens and the functions of *MAT* genes in fungi generally. The presence of a typical mating-type locus that matches the structure and content

of other lichenized fungi suggests that *L. neglecta* may have the genetic capacity to reproduce sexually (Scherrer *et al.* 2005; Wang *et al.* 2016; Aylward *et al.* 2020). If a functional copy of the *MAT1-1* gene is truly missing in this individual, the possibility of primary homothallism can be eliminated, leaving the potential for heterothallism, unisexuality and asexuality to be falsified in this taxon. *Lepraria neglecta* could be heterothallic if a complete *MAT1-1* idiomorph is discovered in a different individual, as was found in *Letharia* spp., *Lobaria pulmonaria* (L.) Hoffm. and many other *Lecanoromycetes* (Honegger *et al.* 2004; Singh *et al.* 2012; Ament-Velásquez *et al.* 2021). The presence of a *MAT1-1-x* pseudogene has been previously observed in *Parmeliaceae*, *Cladoniaceae* and *Umbilicariaceae*, and may not be an anomaly in heterothallic fungi (Armaleo *et al.* 2019; Pizarro *et al.* 2019; Ament-Velásquez 2021). This phenomenon has also been observed in non-lichenized fungi such as *Grosmannia clavigera* (Rob.-Jeffr. & R.W. Davidson) Zipfel *et al.*, in which the *MAT1-2* idiomorph includes a truncated copy of *MAT1-1* (Tsui *et al.* 2013). Alternatively, if the *MAT1-1-x* pseudogene is the only copy of *MAT1-1* in all individuals of *L. neglecta*, the only remaining potential reproductive modes are unisexuality and asexuality. *Neurospora africana* L.H. Huang & Backus, a filamentous ascomycete, was the first described example of unisexuality (Glass & Smith 1994). Similarly, *Huntiella moniliformis* (Hedgc.) Z.W. de Beer *et al.*, another non-lichenized ascomycete, possesses only the *MAT1-2* idiomorph and is capable of unisexual reproduction (Wilson *et al.* 2015*a*). It is unclear whether the remaining hypotheses of sexuality for *Lepraria* spp. are testable and falsifiable. Future research seeking to test these hypotheses may require highly complete genomic resources.

The presence of functional mating-type genes in *L. neglecta* does not necessarily mean that they are capable of sexual reproduction. *MAT1* genes code for transcription factors which can regulate the expression of potentially hundreds of pheromone and pheromone-receptor genes (Pöggeler *et al.* 2006; Bidard *et al.* 2011; Böhm *et al.* 2013; Wilson *et al.* 2021). These downstream pathways have been well characterized in some model fungi but remain unexplored for most taxa. *Fusarium oxysporum* Schltdl. is an ascomycete plant symbiont which uses *MAT*-derived pheromones and autocrine pheromone signalling pathways for density-dependent regulation of conidial sporulation (Vitale *et al.* 2019). *Saccharomyces cerevisiae MAT*-α cells produce α-factor pheromones which induce apoptosis in *MAT*-a cells under certain physiological conditions (Severin & Hyman 2002). The apparently universal conservation of the *MAT1* locus among dikaryotic fungi implies that the *MAT1* genes possess functions essential to species survival. Comparative genomic analysis of more *Lepraria* species and populations will be necessary to begin elucidating the functions of conserved *MAT* genes in this genus of presumed asexual lichens.

Conclusion

Our analysis demonstrates the efficacy of long-read sequencing from heterogeneous metagenomic samples of the lichen symbiosis. With limited time and resources, we produced highly contiguous genomic assemblies, including six of eight nuclear mycobiont chromosomes resolved telomere-to-telomere. We additionally confirmed the presence of an intact mating-type locus in a fungal lineage presumed to be exclusively asexual. Without the need for axenic cultures, long-read sequencing can simultaneously generate genomic data for the mycobiont, photobiont and other symbionts, and rapidly advance our knowledge of lichen biology and fungal genetics.

Author ORCID. Jessica L. Allen, 0000-0002-6152-003X.

References

Allen JL, Jones S and McMullin TR (2021) Draft genome sequence of the lichenized fungus *Bacidia gigantensis*. *American Society for Microbiology* **10**, 1–3.

Altman PL and Dittmer DS (eds) (1972) *Biology Data Book*. 2nd Edn. Bethesda, Maryland: Federation of American Societies for Experimental Biology.

Altschul SF, Gish W, Miller W, Myers EW and Lipman DJ (1990) Basic local alignment search tool. *Journal of Molecular Biology* **215**, 403–410.

Ament-Velásquez SL, Tuovinen V, Bergström L, Spribille T, Vanderpool D, Nascimbene J, Yamamoto Y, Thor G and Johannesson H (2021) The plot thickens: haploid and triploid thalli, hybridization, and biased mating type rations in *Letharia*. *Frontiers in Fungal Biology* **15**, 1–19.

Armaleo D, Müller O, Lutzoni F, Andrésson ÓS, Blanc G, Bode HB, Collart FR, Dal Grande F, Dietrich F, Grigoriev IV, et al. (2019) The lichen symbiosis re-viewed through the genomes of *Cladonia grayi* and its algal partner *Asterochloris glomerata*. *BMC Genomics* **20**, 605–638.

Aylward J, Havnga M, Dreyers LL, Roets F, Wingfield BD and Wingfield MJ (2020) Genomic characterizing of mating type loci and mating type distribution in two apparently asexual plantation tree pathogens. *Plant Pathology* **69**, 28–37.

Bennett RJ and Johnson AD (2003) Completion of a parasexual cycle in *Candida albicans* by induced chromosome loss in tetraploid strains. *EMBO Journal* **22**, 2505–2515.

Bidard FJ, Benkhali A, Coppin E, Imbeaud S, Grognet P, Delacroix H and Debuchy R (2011) Genome-wide gene expression profiling of fertilization competent mycelium in opposite mating types in the heterothallic fungus *Podospora anserina*. *PLoS ONE* **6**, 1–15.

Billiard S, López-Villavicencio M, Hood ME and Girad T (2012) Sex, outcrossing and mating types: unsolved questions in fungi and beyond. *Journal of Evolutionary Biology* **25**, 1020–1038.

Blin K, Shaw S, Kloosterman AM, Charlop-Powers Z, van Wezel GP, Medema MH and Weber T (2021) antiSMASH 6.0: improving cluster detection and comparison capabilities. *Nucleic Acids Research* **49**, W29–W35.

Böhm J, Hoff B, O'Gorman CM, Wolfers S, Klix V, Binger D, Zadra I, Kürnsteiner H, Pöggeler S, Dyer PS, et al. (2013) Sexual reproduction and mating-type-mediated strain development in the penicillin-producing fungus *Penicillium chrysogenum*. *Proceedings of the National Academy of Sciences of the United States of America* **110**, 1476–1481.

Brodo IM, Sharnoff SD and Sharnoff S (2001) *Lichens of North America*. Newhaven & London: Yale University Press.

Chung D, Kwon YM and Yang Y (2021) Telomere-to-telomere genome assembly of asparaginase-producing *Trichoderma simmonsii*. *BMC Genomics* **22**, 1–18.

Clamp M, Cuff J, Searle SM and Barton GJ (2004) The Jalview Java alignment editor. *Bioinformatics* **20**, 426–427.

Crestana GS, Taniguti LM, dos Santos CP, Benevenuto J, Ceresini PC, Carvalho G, Kitajima JP and Monerito-Vitorello CB (2021) Complete chromosome-scale genome sequence resource for *Sprisorium panicileucophaei*, the causal agent of sourgrass smut disease. *Molecular Plant-Microbe Interaction* **34**, 448–452.

Culberson CF and Kristinsson H (1970) A standardized method for the identification of lichen products. *Journal of Chromatography* **46**, 85–93.

D'hondt L, Höfte M, Van Bockstaele E and Leus L (2011) Applications of flow cytometry in plant pathology for genome size determination, detection and physiological status. *Molecular Plant Pathology* **12**, 815–828.

D'Souza CA, Kronstad JW, Taylor G, Warren R, Yuen M, Hu G, Jung WH, Sham A, Kidd SE, Tangen K, *et al.* (2011) Genome variation in *Cryptococcus gatti*, an emerging plant pathogen of immunocompetent hosts. *mBio* **2**, e00342-10.

Edgar RC (2021) MUSCLE v5 enables improved estimates of phylogenetic tree confidence by ensemble bootstrapping. *bioRxiv*. doi: https://doi.org/10.1101/2021.06.20.449169

Gan P, Hiroyama R, Tsushima A, Masuda S, Shibata A, Ueno A, Kumakura N, Narusaka M, Hoat TX, Narusaka Y, *et al.* (2021) Telomeres and a repeat-rich chromosome encode effector gene clusters in plant pathogenic *Colletotrichum* fungi. *Environmental Microbiology* **23**, 1–15.

Glass NL and Smith ML (1994) Structure and function of a mating-type gene from the homothallic species *Neurospora africana*. *Molecular and General Genetics* **244**, 401–409.

Goodwin SB, Ben M'Barek S, Dhillon B, Wittenberg AH, Crane CF, Hane JK, Foster AJ, Van der Lee TA, Grimwood J, Aerts A, *et al.* (2011) Finished genome of the fungal wheat pathogen *Mycosphaerella graminicola* reveals dispensome structure, chromosome plasticity, and stealth pathogenesis. *PLoS Genetics* **7**, e1002070.

Gräser Y, Kuijpers AF, Presber W and Hoog GD (1999) Molecular taxonomy of *Trichophyton mentagrophytes* and *T. tonsurans*. *Medical Mycology* **37**, 315–30.

Grube M, Berg G, Andréson OS, Vilhelmsson O, Dyer PS and Miao VPW (2013) Lichen genomics: prospects and progress. In Martin F (ed.), *The Ecological Genomics of Fungi*. New York: John Wiley & Sons Ltd, pp. 191–212.

Harris RS, Cechova M and Makova KD (2019) Noise-canceling repeat finder: uncovering tandem repeats in error-prone long-read sequencing data. *Bioinformatics* **35**, 4809–4811.

Honegger R, Zippler U, Gassner H and Scherrer S (2004) Mating systems in the genus *Xanthoria* (lichen-forming ascomycetes). *Mycological Research* **108**, 480–488.

Honnay O and Bossuyt B (2005) Prolonged clonal growth: escape route or route to extinction? *Oikos* **108**, 427–432.

Janbon G, Ormerod KL, Paulet D, Byrnes EJ, III, Yadav V, Chatterjee G, Mullapudi N, Honh CC, Billmyre RB, Brunel F, *et al.* (2014) Analysis of the genome and transcriptome of *Cryptococcus neoformans* var. *grubii* reveals complex RNA expression and microevolution leading to virulence attenuation. *PLOS Genetics* **10**, e1004261.

Kalyaanamoorthy S, Minh BQ, Wong TKF, von Haeseler A and Jermiin LS (2017) ModelFinder: fast model selection for accurate phylogenetic estimates. *Nature Methods* **14**, 587–589.

Keepers KG, Pogoda CS, White KH, Anderson Stewart CR, Hoffman JR, Ruiz AM, McCain CM, Lendemer JC, Kane NC and Tripp EA (2019) Whole genome shotgun sequencing detects greater lichen fungal diversity than amplicon-based methods in environmental samples. *Frontiers in Ecology and Evolution* **7**, 1–14.

Kendrick B (2017) *The Fifth Kingdom*. 4th Edn. Ontario: Hackett Publishing.

King R, Urban M, Hammond-Kosack M, Hassani-Pak K and Hammond-Kosack K (2015) The completed genome sequence of the pathogenic ascomycete fungus *Fusarium graminearum*. *BMC Genomics* **16**, 544.

King R, Brown NA, Urban M and Hammond-Kosack K (2018) Inter-genome comparison of the Quorn fungus *Fusarium venenatum* and the closely related plant infecting pathogen *Fusarium graminearum*. *BMC Genomics* **19**, 269.

Kolmogorov M, Yuan J, Lin Y and Pevzner PA (2019) Assembly of long, error-prone reads using repeat graphs. *Nature Biotechnology* **37**, 540–546.

Kooij PW and Pellicer J (2020) Genome size versus genome assemblies: are the genomes truly expanded in polyploid fungal symbionts? *Genome Biology and Evolution* **12**, 2384–2390.

Kramer GJ and Nodwell JR (2017) Chromosome level assembly and secondary metabolite potential of the parasitic fungus *Cordyceps militaris*. *BMC Genomics* **18**, 1–10.

Li H (2018) Minimap2: pairwise alignment for nucleotide sequences. *Bioinformatics* **34**, 3094–3100.

Lendemer JC (2013) A monograph of the crustose members of the genus *Lepraria* Ach. s. str. (*Stereocaulaceae*, lichenized *Ascomycetes*) in North America north of Mexico. *Opuscula Philolichenum* **12**, 27–141.

Lendemer JC and Hodkinson BP (2013) A radical shift in the taxonomy of *Lepraria* s.l.: molecular and morphological studies shed new light on the evolution of asexuality and lichen growth form diversification. *Mycologia* **105**, 994–1018.

Machida M, Asai K, Sano M, Tanaka T, Kumagai T, Terai G, Kusumoto K, Arima T, Akita O, Kashiwagi K, *et al.* (2005) Genome sequencing and analysis of *Aspergillus oryzae*. *Nature* **438**, 1157–1161.

Manni M, Berkeley MR, Seppey M, Simão FA and Zdobnov FM (2021) BUSCO update: novel and streamlined workflows along with broader and deeper phylogenetic coverage for scoring of eukaryotic, prokaryotic, and viral genomes. *Molecular Biology and Evolution*, **38**, 4647–4654.

McKenzie SK, Walston RF and Allen JL (2020) Complete, high-quality genomes from long-read metagenomic sequencing of two wolf lichen thalli reveals enigmatic genome architecture. *Genomics* **112**, 3150–3156.

Meiser A, Otte J, Schmitt I and Dal Grande F (2017) Sequencing genomes from mixed DNA samples – evaluating the metagenome skimming approach in lichenized fungi. *Scientific Reports* **7**, 14881.

Mikheenko A, Prjibelski A, Saveliev V, Antipov D and Gurevich A (2018) Versatile genome assembly evaluation with QUAST-LG. *Bioinformatics* **34**, i142–i150.

Muggia L, Kopun T and Grube M (2017) Effects of growth media on the diversity of culturable fungi from lichens. *Molecules* **22**, 824.

Nguyen LT, Schmidt HA, von Haeseler A and Minh BQ (2015) IQ-TREE: a fast and effective stochastic algorithm for estimating maximum likelihood phylogenies. *Molecular Biology and Evolution* **32**, 268–274.

Olarte RA, Menke J, Zhang Y, Sullivan S, Slot JC, Huang Y, Badalamenti JP, Quandt AC, Spatafora JW and Bushley KE (2019) Chromosome rearrangements shape the diversification of secondary metabolism in the cyclosporin producing fungus *Tolypocladium inflatum*. *BMC Genomics* **20**, 1–23.

Park S-Y, Choi J, Kim JA, Jeong M-H, Kim S, Lee Y-H and Hur J-S (2013*a*) Draft genome sequence of *Cladonia macilenta* KoLRI003786, a lichen-forming fungus producing biruloquinone. *Genome Announcements* **1**, e00695–13.

Park S-Y, Choi J, Kim JA, Yu N-H, Kim S, Kondratyuk SY, Lee Y-H and Hur J-S (2013*b*) Draft genome sequence of lichen-forming fungus *Caloplaca flavorubescens* strain KoLRI002931. *Genome Announcements* **1**, e00678–13.

Park S-Y, Choi J, Lee G-W, Kim JA, Oh S-O, Jeong M-H, Yu N-H, Kim S, Lee Y-H and Hur J-S (2014*a*) Draft genome sequence of lichen-forming fungus *Cladonia metacorallifera* strain KoLRI002260. *Genome Announcements* **2**, e01065–13.

Park S-Y, Choi J, Lee G-W, Jeong M-H, Kim JA, Oh S-O, Lee Y-H and Hur J-S (2014*b*) Draft genome sequence of *Umbilicaria muehlenbergii* KoLRILF000956, a lichen-forming fungus amenable to genetic manipulation. *Genome Announcements* **2**, e00357–14.

Patwardhan PG and Badhe PD (1978) Development of ascocarp and cytology of ascus in *Dermatocarpon moulinsii* (Mont.). *Indian Journal of Botany* **1**, 117–126.

Persinoti GF, Martinez DA, Li W, Dögen A, Billmyre RB, Averette A, Goldberg JM, Shea T, Young S, Zeng Q, *et al.* (2018) Whole-genome analysis illustrates global clonal population structure of the ubiquitous dermatophyte pathogen *Trichophyton rubrum*. *Genetics* **208**, 1657–1669.

Pizarro D, Dal Grande F, Leavitt SD, Dyer PS, Schmitt I, Crespo A, Lumbsch HT and Divakar PK (2019) Whole-genome sequence data uncover widespread heterothallism in the largest group of lichen-forming fungi. *Genome Biology and Evolution* **11**, 721–730.

Pöggeler S, Nowrousian M, Ringelberg C, Loros JJ, Dunlap JC and Kück U (2006) Microarray and real-time PCR analyses reveal mating type-dependent gene expression in a homothallic fungus. *Molecular Genetics and Genomics* **275**, 492–503.

Poma A, Pacioni G, Ranalli R and Miranda M (1998) Ploidy and chromosomal number in *Tuber aestivum*. *FEMS Microbiology Letters* **167**, 101–105.

Rautiainen M and Marschall T (2020) GraphAligner: rapid and versatile sequence-to-graph alignment. *Genome Biology* **21**, 253.

Rossen JM and Westergaard M (1966) Studies on the mechanism of crossing over. II. Meiosis and the time of meiotic chromosome replication in the ascomycete *Neottiella rutilans* (Fr.) Dennis. *Comptes-Rendus des Travaux du Laboratoire Carlsberg* **35**, 233–260.

Scherrer S, Zippler U and Honegger R (2005) Characterisation of mating-type locus in the genus *Xanthoria* (lichen-forming ascomycetes, *Lecanoromycetes*) *Fungal Genetics and Biology* **42**, 976–988.

Severin FF and Hyman AA (2002) Pheromone induces programmed cell death in *Saccharomyces cerevisiae*. *Current Biology* **12**, R233–R235.

Singh G, Dal Grande F, Cornejo C, Schmitt I and Scheidegger C (2012) Genetic basis of self-incompatibility in the lichen-forming fungus *Lobaria pulmonaria* and skewed frequency distribution of mating-type idiomorphs: implications for conservation. *PLoS ONE* **7**, 1–9.

Smith SE and Read DJ (2008) *Mycorrhizal Symbiosis*. 3rd Edn. Cambridge, Massachusetts: Academic Press.

Specht T, Dahlmann TA, Zadra I, Kürnsteiner H and Kück U (2014) Complete sequencing and chromosome-scale genome assembly of the industrial progenitor strain P2niaD18 from the penicillin producer *Penicillium chrysogenum*. *Genome Announcements* **2**, e00577–14.

Stajich JE, Berbee ML, Blackwell M, Hibbett DS, James TY, Spatafora JW and Taylor JW (2009) The Fungi. *Current Biology* **19**, R840–R845.

Talhinhas P, Tavares D, Ramos AP, Goncalves S and Loureiro J (2017) Validation of standards suitable for genome size estimation of fungi. *Journal of Microbiological Methods* **142**, 76–78.

Tedersoo L, Sánchez-Ramírez S, Kõljalg U, Bahram M, Döring M, Schigel D, May T, Ryberg M and Abarenkov K (2018) High-level classification of the *Fungi* and a tool for evolutionary ecological analyses. *Fungal Diversity* **90**, 135–159.

Tedersoo L, Albertsent M, Anslan S and Callahan B (2021) Perspectives and benefits of high-throughput long-read sequencing in microbial ecology. *Applied Environmental Microbiology* **87**, e00626–21.

Thomson GJ, Hernon C, Austriaco N, Shapiro RS, Belenky B and Bennett RJ (2019) Metabolism-induced oxidative stress and DNA damage selectively trigger genome instability in polyploid fungal cells. *EMBO Journal* **38**, e101597.

Thorvaldsdóttir H, Robinson JT and Mesirov JP (2013) Integrative Genomics Viewer (IGV): high-performance genomics data visualization and exploration. *Briefings in Bioinformatics* **14**, 178–192.

Thüs H, Muggia L, Pérez-Ortega S, Favero-Longo SE, Joneson S, O'Brien H, Nelsen MP, Duque-Thüs R, Grube M, Friedl T, *et al.* (2011) Revisiting photobiont diversity in the lichen family *Verrucariaceae* (Ascomycota). *European Journal of Phycology* **46**, 399–415.

Tillich M, Lehwark P, Pellizzer T, Ulbricht-Jones ES, Fischer A, Bock R and Greiner S (2017) GeSeq – versatile and accurate annotation of organelle genomes. *Nucleic Acids Research* **45**, W6–W11.

Tischler G (1922) *Allgemeine Pflanzenkaryologie, Vol. 2.* Berlin: Gebrüder Bontraeger.

Tripp EA (2016) Is asexual reproduction an evolutionary dead end in lichens? *Lichenologist* **48**, 559–580.

Tsui CKM, Diguistini S, Wang Y, Feau N, Dhillon B, Bohlmann J and Hamelin RC (2013) Unequal recombination and evolution of the mating-type (*MAT*) loci in the pathogenic fungus *Grosmannia clavigera* and relatives. *G3* **3**, 465–480.

Tzovaras G, Segers FH, Bicker A, Dal Grande F, Otte J, Anvar SY, Hankeln T, Schmitt I and Ebersberger I (2020) What is in *Umbilicaria pustulata*? A metagenomic approach to reconstruct the holo-genome of a lichen. *Genome Biology and Evolution* **12**, 309–324.

Vitale S, Pietro AD and Turrà D (2019) Autocrine pheromone signaling regulates community behavior in the fungal pathogen *Fusarium oxysporum*. *Nature Microbiology* **4**, 1443–1449.

Wang B, Liang X, Gleason ML, Hsiang T, Zhang R and Sun G (2020) A chromosome-scale assembly of the smallest Dothideomycete genome reveals a unique genome compaction mechanism in filamentous fungi. *BMC Genomics* **21**, 1–13.

Wang Q, Wang S, Xiong CL, James TY and Zhang XG (2016) Mating-type genes of the anamorphic fungus *Ulocladium botrytis* affect both asexual sporulation and sexual reproduction. *Scientific Reports* **7**, 1–12.

Wang Y, Yuan X, Chen L, Wang X and Li C (2018) Draft genome sequence of the lichen-forming *Ramalina intermedia* strain YAF0013. *Genome Announcements* **6**, e00478–18.

Wilson AM, Gondlonton T, van der Nest MA, Wilken PM, Wingfield MJ and Wingfield BD (2015a) Unisexual reproduction in *Huntiella moniliformis*. *Fungal Genetics and Biology* **80**, 1–9.

Wilson AM, Wilken PM, van der Nest MA, Steenkamp ET, Wingfield MJ and Wingfield BD (2015b) Homothallism: an umbrella term for describing diverse sexual behaviours. *IMA Fungus* **6**, 207–214.

Wilson AM, Gabriel R, Singer SW, Schuerg T, Wilken PM, van der Nest MA, Wingfield MJ and Wingfield BD (2021) Doing it alone: unisexual reproduction in filamentous ascomycete fungi. *Fungal Biology Reviews* **35**, 1–13.